Optica Applicata, Vol. XLI, No. 1, 2011

Determination of optical constants and thickness of amorphous GaP thin film

NUWAT PIMPABUTE[1], THANUSIT BURINPRAKHON[1*], WEERASAK SOMKHUNTHOT[2]

[1]Department of Physics, Faculty of Science, Khon-Kaen University, Khon-Kaen, 40002, Thailand

[2]Department of General Sciences, Faculty of Sciences and Technology, Loei Rajabhat University, Loei, 42001, Thailand

[*]Corresponding author: thanusit@kku.ac.th

Gallium phosphide (GaP) thin film was prepared by an asymmetric bipolar pulsed-dc magnetron sputtering technique onto glass substrate at room temperature in an Ar atmosphere. A compacted GaP powder was used as a target. The X-ray diffraction patterns show that the film is amorphous. The transmittance of the film was measured in the incident photon wavelength range of 300–2000 nm. The film's refractive index, thickness and absorption coefficient as a function of wavelength were determined by using Swanepoel's method. The deduced absorption data indicate that the optical transition in the film is dominated by the indirect type. The corresponding energy of 1.51 eV was obtained for the 563±16 nm thin film.

Keywords: pulsed dc sputtering, gallium phosphide film, optical constants, optical band gap.

1. Introduction

Gallium phosphide is one of the most important group III–V compounds which has been extensively developed for applications to optical devices, LEDs, photo cells, *etc*. It has been found to be important for light emission devices in visible range [1] and it is one of the most promising materials for development of solar cells [2]. Amorphous gallium phosphide (a-GaP) has also been developed for wide-area and low cost devices in the same manner as amorphous silicon [3, 4]. In the form of a thin film, a-GaP has been prepared using a variety of methods, such as plasma metallic organized chemical vapor deposition [5], ion beam assistant deposition [6] and reactive rf sputtering [7], *etc*. The optical properties of the film depend strongly on preparation methods and conditions.

Among these preparation methods, sputtering is the most common method used for preparing optical thin films because it enables variation of the deposition parameters so that films with required physical and optical properties can be obtained [8]. Pulsed dc magnetron sputtering is a relatively new sputtering method that has been used for thin film preparation. Pulsing the magnetron discharge in the mid frequency range

(10–200 kHz) stabilizes plasma, prevents arcing and yields high deposition rates [9]. It is thus very interesting to investigate optical properties of a-GaP thin films obtained from pulsed dc magnetron sputtering and compare them to other methods.

For the optical property assessment of thin films, there have been various methods for determining the optical constants and thickness of the films, such as the classical oscillator fit procedure, the Kramers–Kronig analysis and the Swanepoel method [10, 11]. The last is widely used because it enables the determination of the refractive index and other optical constants of thin films from only the normal incident optical transmission spectrum [12].

In this article, we report the application of the Swanepoel method to determine the refractive index, thickness, absorption coefficient and energy gap of a-GaP thin film deposited by asymmetric pulsed-dc magnetron sputtering onto a glass substrate. Results compared to those of a-GaP obtained by other deposition techniques are presented.

2. Swanepoel's method

2.1. Optical transmission spectrum of film/transparent substrate system

Figure 1 shows schematically the optical transmission measurement on a film/substrate system, in which the substrate is transparent and the film is semitransparent or transparent, and the finite thickness of the substrate d_s is several orders of magnitude larger than the film thickness d. Assuming normal incident and taking into account interference due to multiple refractions at film/substrate and air/film interfaces, SWANEPOEL [11] has shown that the total transmission $T(\lambda)$ is given by,

$$T(\lambda) = \frac{Ax}{B - Cx\cos\varphi + Dx^2} \tag{1}$$

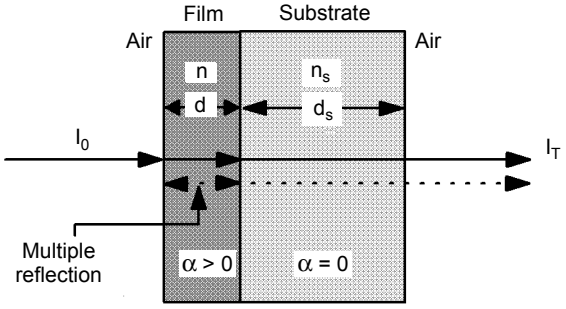

Fig. 1. Schematic diagram of light transmission through a film/substrate system. I_0 is the intensity of the normal incident beam. I_T is the total intensity of transmitted beams, which is the superposition of the directly transmitted beams (solid line) and the beams transmitted after undergoing multiple reflections at the air/film and film/substrate interfaces (dashed line). In this model, transmittance is defined as $T = I_T/I_0$.

where

$$A = 16n^2 n_s \tag{2a}$$

$$B = (n+1)^3\left(n + n_s^2\right) \tag{2b}$$

$$C = 2(n^2-1)\left(n^2 - n_s^2\right) \tag{2c}$$

$$D = (n-1)^3\left(n - n_s^2\right) \tag{2d}$$

$$\varphi = \frac{4\pi nd}{\lambda} \tag{2e}$$

$$x = \exp(-\alpha d) \tag{2f}$$

where n is the refractive index of the film, n_s is the refractive index of the substrate, d is the thickness, φ is the phase difference between the direct and the multiple reflected transmitted beams, x is the absorbance and α is the absorption coefficient.

The transmission spectrum according to the above expression for a-Si:H is shown in Fig. 2.

The extremes of $T(\lambda)$ in Eq. (1) occur for $\varphi = 2m\pi$ or

$$2nd = m\lambda \tag{3}$$

where m is an integer for maxima and a half integer for minima. The transmittance for maxima and minima are therefore given by:

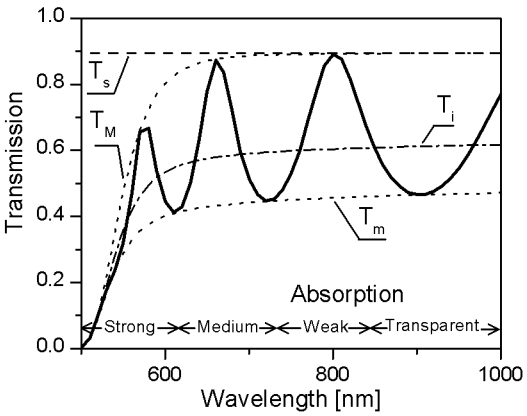

Fig. 2. Simulated transmission spectra (solid line) of a-Si:H and a clean substrate T_s. The film thickness of 600 nm, n_s of 1.6, and the same $n(\lambda)$ and $\alpha(\lambda)$ as in Ref. [10] are assumed. The envelopes T_M, T_m and the smooth curve T_i are constructed from polynomial equations, respectively.

$$T_M = \frac{Ax}{B - Cx + Dx^2} \tag{4}$$

$$T_m = \frac{Ax}{B + Cx + Dx^2} \tag{5}$$

T_M and T_m, when considered as smooth functions of λ, define the envelopes passing tangentially through the maxima and minima, as shown in Fig. 2. Constructing the two envelopes for the experimental transmission spectrum of a film/substrate sample and knowing transmission of the clean substrate alone make possible the determination of the refractive index and absorption coefficient of the film. This will be briefly detailed in Sections 2.2 and 2.3.

2.2. Determination of refractive index and thickness

Assuming the two envelopes are known, subtracting the reciprocal of Eq. (5) from that of Eq. (4) at any λ above the strong absorption region (see Fig. 2) yields the equation that is independent of the absorbance x [11]:

$$\frac{1}{T_m} - \frac{1}{T_M} = \frac{2C}{A} \tag{6}$$

Substituting the expression of A and C from Eq. (2) and solving for n yields,

$$n = \sqrt{N + \sqrt{N^2 - n_s^2}} \tag{7}$$

where

$$N = 2n_s \frac{T_M - T_m}{T_M T_m} + \frac{n_s^2 + 1}{2} \tag{8}$$

and n_s is the refractive index of the substrate and can be calculated from the transmission spectrum of a clean substrate (T_s) via the relation [13]

$$n_s = \frac{1}{T_s} + \sqrt{\frac{1}{T_s^2} - 1} \tag{9}$$

Equation (7) leads to the refractive index of the film at the sampled λ. If the refractive indices are obtained at the maxima or minima of the transmission spectrum, the thickness of the film can be deduced. Let n_1 and n_2 be refractive indices at two adjacent maxima (or minima) at λ_1 and λ_2, $\lambda_1 > \lambda_2$, it follows from Eq. (3) that:

$$2n_1 d = m\lambda_1 \tag{10}$$

$$2n_2 d = (m + 1)\lambda_2 \tag{11}$$

Solving Eqs. (10) and (11) for d yields the film thickness as [14]:

$$d = \frac{\lambda_1 \lambda_2}{2(\lambda_1 n_2 - \lambda_2 n_1)} \tag{12}$$

Practically, there will be errors in the determination of extreme positions and the corresponding values of the smooth envelopes T_M and T_m. Therefore, the preliminary values of the refractive index calculated from Eq. (7) and the film thickness obtained from Eq. (12), to be denoted respectively by n_{pre} and d_{pre}, are inaccurate. The more accurate thickness and refractive index can be obtained by further performing the following steps. Firstly, take the average value of d_{pre} obtained from each two adjacent maxima (or minima). Secondly, use Eq. (3) to determine the estimated order number (m_{est}) for each extreme from the average value of d_{pre} and n_{pre} and round off each resulting m_{est} to the closest integer for maxima or half integer for minima. These round values will be considered as the exact order number m_{exact} corresponding to each maxima or minima. Thirdly, use m_{exact} and n_{pre} again to calculate the accurate thickness d_{accurate} for each maxima and minima. The average value of d_{accurate} will be taken as the final thickness of the film. Finally, from the exact value of m and the final thickness of the film, the accurate refractive index n_{accurate} can again be calculated for each maximum and minimum using Eq. (3). The refractive index as a function of wavelength $n(\lambda)$ can be then obtained by fitting the experimentally evaluated values to an appropriate model. In this work, the Sellmeier equation used by POELMAN and SMET [15] is employed.

$$n = \sqrt{a + \frac{b\lambda^2}{\lambda^2 - c^2}} \tag{13}$$

where a, b, c are fitting parameters of the Sellmeier equation.

2.3. Absorption coefficient determination

Once $n(\lambda)$ and accurate thickness are obtained and the refractive index of the substrate is known, the constants A, B, C and D in Eq. (1) can be calculated according to Eqs. (2a)–(2d). Then, the absorbance x as a function of wavelength $x(\lambda)$ can be calculated as follows. The addition of the reciprocal of Eqs. (4) and (5) at defined above gives [16]:

$$\frac{1}{T_M} + \frac{1}{T_m} = \frac{2(B + Dx^2)}{Ax} \tag{14}$$

or

$$(T_i D)x^2 - Ax + T_i B = 0 \tag{15}$$

Solving the above quadratic Eq. (14) for x, we will have,

$$x = \frac{A - \sqrt{A^2 - 4T_i^2 BD}}{2T_i D} \tag{16}$$

where

$$T_i = \frac{2T_M T_m}{T_M + T_m} \tag{17}$$

The term T_i represents the curve which is a close approximation to the interference--free transmission of the film. In the strong absorption region, the value of $T_i(\lambda)$ can be estimated to be $T(\lambda)$. Above the strong absorption region, the values of T_i at the maxima and minima can be calculated from the corresponding T_M and T_m using Eq. (17). Fitting these experimental data of $T_i(\lambda)$ using a polynomial interpolation yields the continuous $T_i(\lambda)$. Once the smooth function $T_i(\lambda)$ is obtained, the wavelength dependent absorbance $x(\lambda)$ can be calculate from Eq. (16) and the absorption coefficient as a function of wavelength $\alpha(\lambda)$ can be calculated using Eq. (2f) rewritten in the form of:

$$\alpha(\lambda) = -\frac{\ln\left[x(\lambda)\right]}{\overline{d}_{\text{accurate}}} \tag{18}$$

where $\overline{d}_{\text{accurate}}$ is the average value of the accurate thickness described above.

3. Experimental details

The deposition of GaP thin films was carried out using an in-house-built asymmetric pulsed-dc magnetron sputtering system [17]. The sputtering target was made of GaP powder pressed to in a circular copper base. The diameter and the thickness of the compacted powder were 6.00 cm and 0.25 cm, respectively. The glass slide was used as a substrate and the deposition area of 1.20×1.20 cm^2 on the substrate was obtained by means of an aluminium mask. The substrate was placed at a distance of 6.00 cm above the target and no additional heating was applied. To generate the pulsed-dc plasma and initiate the thin film deposition, the vacuum chamber was pumped down to a base pressure of 15 mT and flushed with high purity argon (Ar 99.999%) for several cycles to ensure the cleanliness of the chamber. The pulsed-dc Ar plasma was generated at an argon gas pressure of 70 mTorr and

a pulse frequency of 17 kHz, a negative sputtering voltage of –850 V, and a positive reverse voltage of 100 V. The thin film was deposited for 10 minutes.

The crystal structure of the deposited film was investigated by X-ray diffractometer equipped with CuK_α radiation, $\lambda = 0.15406$ nm. The grazing XRD measurement with an incident angle of 3° was used to eliminate the contribution of the glass substrate to the XRD pattern. The thickness of the film was measured using Veeco Dektak 150 surface profiler for comparison of the calculated values of thickness.

The optical transmission spectrum of the film was obtained via UV–VIS–NIR spectrophotometer (UV-3101 PC, Shimadzu Ltd., Japan) at room temperature in the range of 300–2000 nm. The relative uncertainty in the transmittance is 0.3%. In the measurement, air was used as a reference.

4. Results and discussion

4.1. Structural properties

Figure 3 shows the glazing XRD pattern of the GaP film compared to the XRD of a glass substrate obtained from a normal θ–2θ scan. The XRD pattern of the film shows two broad peaks centered around at 2θ of 28° and 52°, indicating an amorphous nature or extremely fine crystalline size of the film.

4.2. Transmission spectra

Figure 4 shows the optical transmission spectra of the clean glass substrate and the pulsed-dc sputtering a-GaP thin film deposited on the substrate. The transmittance of the substrate, T_s, is around 90% in the range of 350–2000 nm, indicating a highly transparent material. The optical transmission spectrum of the a-GaP film/substrate, $T(\lambda)$, shows an absorption edge around 600 nm and exhibits appreciable interference fringes in the region of 700–2000 nm. The spectrum structure is similar to the medium and strong absorption regions of the simulated spectrum in Fig. 2. Therefore, it is

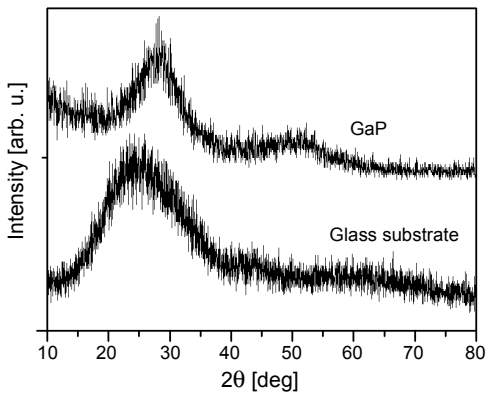

Fig. 3. XRD patterns of pulsed-dc sputtering deposited a-GaP film and the glass substrate.

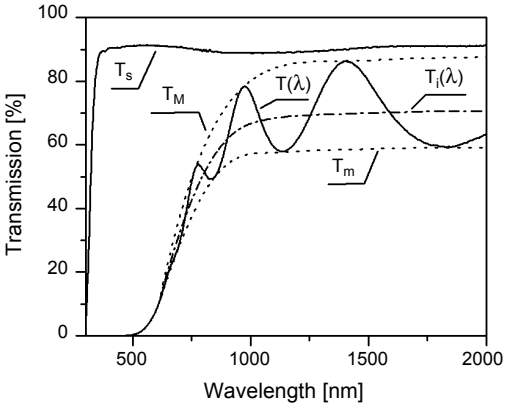

Fig. 4. Optical transmission spectra of a clean glass substrate, T_s, and that of the pulsed-dc sputtering a-GaP thin film on the substrate, $T(\lambda)$. T_M, T_m are constructed envelopes for maxima and minima and $T_i(\lambda)$ is a smooth curve evaluated from T_M, T_m.

justified that the transmission spectrum of the film/substrate system under investigation can be analyzed using the Swanepoel method described in Section 2.

4.3. Determination of refractive index and thickness

To determine the refractive index and the film thickness, the procedure described in Sections 2.1 and 2.2 are followed. The two envelopes are constructed, as shown in Fig. 4, using smoothing average method. The wavelengths at the maxima and minima and the corresponding T_M and T_m are read out and listed in column 1, 2, and 3 of the Table, respectively. In the 4-th column of the Table, the refractive indices of the substrate at λ for the extremes determined using Eq. (13) are given. From these data, the corresponding values of n_{pre}, d_{pre}, m_{est}, m_{exact} and d_{accurate} at each maxima and

T a b l e. Values of various parameters obtained in the process of the determination of refractive index and thickness of a-GaP thin film. The bold-face values in T_M and T_m are values at maxima and minima, respectively. (To be continued on next page.)

λ [nm]	T_M	T_m	n_s	n_{pre}	d_{pre} [nm]
1	2	3	4	5	6
1842.4	0.882±0.003	0.594±0.002	1.55±0.01	2.54±0.01	567
1407.2	0.861±0.003	0.590±0.002	1.60±0.01	2.56±0.01	607
1143.2	0.829±0.002	0.580±0.002	1.64±0.01	2.58±0.01	643
975.6	0.781±0.002	0.557±0.002	1.64±0.01	2.58±0.01	650
852.4	0.673±0.002	0.496±0.001	1.63±0.01	2.59±0.01	–
772.0	0.546±0.002	0.413±0.001	1.60±0.01	2.64±0.01	–
				$\overline{d}_{\text{pre}}$	617
				σ	±38

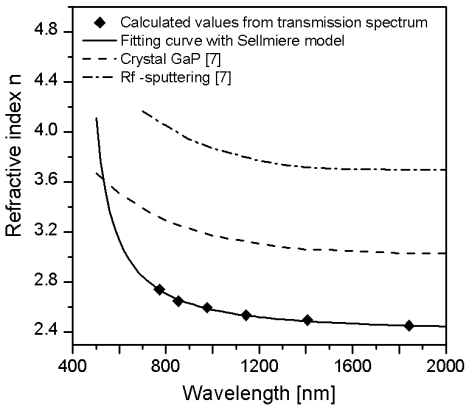

Fig. 5. The refractive index of the pulsed-dc sputtering deposited a-GaP film compared to those of a-GaP film deposited by rf-sputtering and crystalline GaP [7]. The dots are the values calculated from the transmission spectrum. The solid line is the fitted curve using Sellmeier equation expressed by: $n(\lambda) = \sqrt{2.102 + 3.689\lambda^2/(\lambda^2 - 432^2)}$.

minima were obtained as given in columns 5 to 9 of the Table, respectively. The error of the average thickness significantly improved from ±38 for d_{pre} to ±16 for d_{accurate}. The final thickness of 563±16 nm is obtained, which is comparable to the value of 488±29 nm measured by a surface step profiler. The accurate refractive index n_{accurate} at the λ for each maxima and minima was obtained from m_{exact} and the final thickness using Eq. (3) again, see column 10 of the Table. Finally, the refractive index as a function of wavelength, $n(\lambda)$, was obtained by fitting the values for the maxima and minima to the Sellmeier model given in Eq. (13). The result is shown in Fig. 5, indicating a good fit. In the wavelength range above 700 nm, it is clearly seen from the figure that the refractive index of the present a-GaP film is lower than that of crystalline GaP and rf-sputtered a-GaP films. This could be due to the different physical environment in the pulsed-dc and the rf-sputtering.

T a b l e. Continued.

m_{est}	m_{exact}	d_{accurate} [nm]	n_{accurate}
7	8	9	10
1.70	1.5	586	2.45±0.07
2.24	2.0	576	2.50±0.07
2.78	2.5	567	2.54±0.07
3.26	3.0	553	2.60±0.08
3.74	3.5	549	2.65±0.08
4.21	4.0	545	2.74±0.08
	$\overline{d}_{\text{accurate}}$	563	
	σ	±16	

4.4. Determination of optical absorption coefficient

From the $n(\lambda)$ obtained in the previous section and the smooth function $T_i(\lambda)$ constructed as shown in Fig. 4, the optical absorption coefficient as a function of wavelength of the pulsed-dc sputtering deposited film was obtained using the procedure described in Section 2.3. The result is given in Fig. 6. It can be seen that the absorption coefficient of the a-GaP film under this investigation exhibits a close trend and magnitude to that of the plasma metallic organized chemical vapor deposited (MOCVD) a-GaP film, reported by KNIGHTS and LUJAN [5]. However, the values in

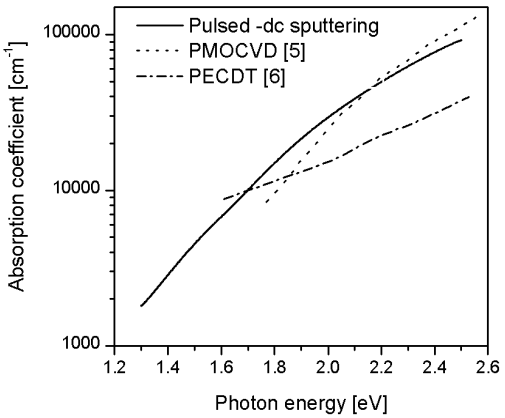

Fig. 6. Absorption coefficient of sputtered a-GaP film compared to that of a-GaP films from MOCVD and PECTD methods.

the visible region are about 2–3 times as high as those of plasma enhanced chemical transport deposited (PECTD) a-GaP film of XU JIANHONG *et al*. [6]. This indicates the different internal structure of a-GaP films obtained from different deposition techniques.

4.5. Optical energy gap determination

The type of allowed optical transitions in a semiconductor and the optical band gap can be evaluated by observing the absorption coefficient as a function of the photon energy using Tauc's law [18]:

$$(\alpha h\nu)^m = B\left(h\nu - E_g\right) \tag{19}$$

where B is a constant, E_g is the optical energy gap and m is a constant which determines the type of the optical transition (m = 2 and 1/2 for direct allowed transition and indirect allowed transition, respectively).

The plots of $(\alpha h\nu)^{1/2}$ and $(\alpha h\nu)^2$ versus $h\nu$ in the strong and medium absorption regions are shown in Fig. 7. A linear region over a wide range of photon energy was found in a plot of $(\alpha h\nu)^{1/2}$ *vs*. $h\nu$, indicating that the dominant transition type is indirect [19]. Therefore, the optical energy gap of the film was determined by assuming

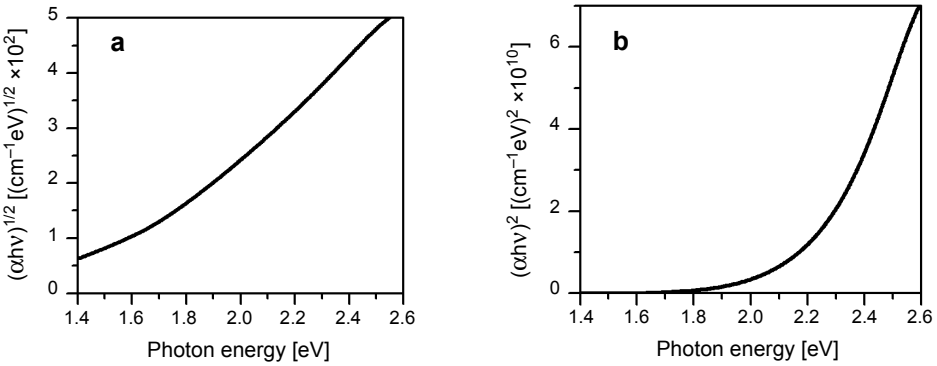

Fig. 7. Plots of $(\alpha h\nu)^{1/2}$ *vs.* $h\nu$ (**a**) and $(\alpha h\nu)^2$ *vs.* $h\nu$ (**b**) of the pulsed-dc sputtering a-GaP.

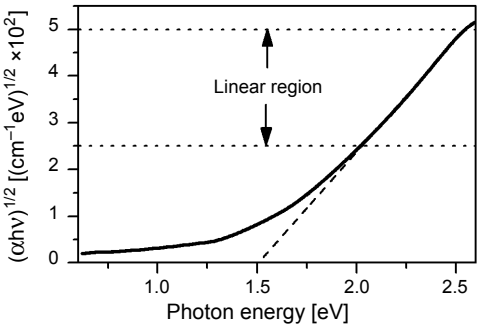

Fig. 8. A plot of $(\alpha h\nu)^{1/2}$ versus the incident photon energy $h\nu$ of a-GaP film.

indirect transition and interpolating the linear portion of the plot of $(\alpha h\nu)^{1/2}$ *vs.* $h\nu$ (see Fig. 8). The value of optical energy gap was about 1.51 eV which is close to 1.6 eV reported by XU JIANHONG *et al*. [6] for the PECTD a-GaP film.

5. Conclusions

Thin film of a-GaP was deposited onto a glass substrate at room temperature using a pulsed-dc magnetron sputtering technique. The as-deposited film was amorphous. The optical constants as a function of wavelength, such as refractive index n, absorption coefficient α and the thickness of the film were evaluated from the optical transmission spectrum using Swanepoel's method. The film thickness obtained from the model is comparable to that measured directly from the nano-step profiler. The refractive index of the film can be fitted to the Sellmeier equation. The film exhibits indirect optical transition with an optical band gap of 1.51 eV.

Acknowledgements – This work was financially supported by the Office of the Higher Education Commission (Ministry of Education), Physics Department, Khon Kaen University and Loei Rajabhat University, Thailand.

References

[1] HATAMI F., MASSELINK W.T., LORDI V., HARRIS J.S., *Green emission from InP–GaP quantum-dot light-emitting diode*, IEEE Photonics Technology Letters **18**(7), 2006, pp. 895–897.

[2] EPSTEIN A.S., GROVE W.O., *Single crystal gallium phosphide solar cells*, Advance Energy Conversion **5**(2), 1965, pp. 161–172.

[3] KUBOTA H., MATSUMOTO T., HARAYU T., FUJIYOSHI T., MIYAGAV R., MIYAHARA K., *Amorphous gallium phosphide (a-GaP) pn-diode by ion beam assisted deposition*, International Photovoltaic Science and Engineering Conference **35**(7), 1994, pp. 353–358.

[4] KUMABE K., MATSUMOTO N., *Properties of GaAs and GaP amorphous-film/crystal junctions*, Japanese Journal of Applied Physics **18**(9), 1979, pp. 1789–1794.

[5] KNIGHTS J.C., LUJAN R.A., *Plasma deposition of GaP and GaN*, Journal of Applied Physics **49**(3), 1978, pp. 1291–1293.

[6] XU JIANHONG, CHEN KUNJI, ZHU ENJUN, *Investigation of optical properties of amorphous GaP films*, Chinese Physics Letters **8**(4), 1991, pp. 187–190.

[7] MATSUMOTO N., KUMABE K., *Effects of hydrogen incorporation during deposition by sputtering for amorphous gallium phosphide films*, Japanese Journal of Applied Physics **18**(5), 1979, pp. 1011–1012.

[8] REINIG R., ALEX V., FENSKE F., FUHS W., SELLE B., *Pulsed dc magnetron-sputtering of microcrystalline silicon*, Thin Solid Films **403–404**, 2002, pp. 86–90.

[9] KELLY P.J., ARNELL R.D., *Magnetron sputtering: A review of recent developments and applications*, Vacuum **56**(3), 2000, pp. 159–172.

[10] DURMUS H., SAFAK H., KARABIYIK H., *Determination of optical constant of materials by two different methods: An application to single crystals Si*, Turkish Journal of Physics **24**(6), 2000, pp. 725–735.

[11] SWANEPOEL R., *Determination of the thickness and optical constants of amorphous silicon*, Journal of Physics E: Scientific Instruments **16**(12), 1983, pp. 1214–1222.

[12] THAKUR A., SHARMA V., SAINI G.S.S., GOYAL N., TRIPATHI S.K., *Calculation of optical parameters of a-Ge-Se-Sn thin films*, Journal of Optoelectronics and Advanced Materials **7**(4), 2005, pp. 2077–2083.

[13] NICA V., CHIRA S., MADARE D., *Determination of the optical constants and thickness of titanium oxide thin films by Swanepoel method*, Fizica Staii Condensate **LI–LII**, 2005–2006, pp. 184–191.

[14] BAKRY A.M., *Influence of film thickness on the optical properties of hydrogenated amorphous silicon thin films*, Egyptian Journal of Solids **31**(1), 2008, pp. 11–22.

[15] POELMAN D., SMET P.F., *Methods for the determination of the optical constants of thin films from single transmission measurements: A critical review*, Journal of Physics D: Applied Physics **36**(15), 2003, pp. 1850–1857.

[16] ILKER A., HUSEYIN T., *Optical transmission measurements on glow-discharge amorphous silicon nitride films*, Turkish Journal of Physics **25**(3), 2001, pp. 215–222.

[17] SOMKHUNTHOT W., BURINPRAKHON T., THOMAS I., SEETAWAN T., AMORNKITBAMRUNG V., *Bipolar pulsed-DC power supply for magnetron sputtering and thin films synthesis*, Elektrika **9**(2), 2007, pp. 20–26.

[18] YUE G.H., PENG D.L., YAN P.X., WANG L.S., WANG W., LUO X.H., *Structure and optical properties SnS thin film prepared by pulse electrodeposition*, Journal of Alloys and Compounds **468**(1–2), 2009, pp. 254–257.

[19] ILICAN S., ZOR M., CAGLAR Y., CAGLAR M., *Optical characterization of the $CdZn(S_{1-x}Se_x)_2$ thin films deposited by spray pyrolysis method*, Optica Applicata **36**(1), 2006, pp. 29–37.

Received March 23, 2010
in revised form August 31, 2010